Vacuum 212 (2023) 112031

Contents lists available at ScienceDirect

Vacuum

journal homepage: www.elsevier.com/locate/vacuum

Mass Spectrometric study of graphene-oxide irradiated in vacuum by Nd: YAG laser

L. Torrisi [a,c,*], M. Cutroneo [b], L. Silipigni [a,c], A. Torrisi [d]

[a] Dip.to di Scienze Matematiche e Informatiche, Scienze Fisiche e Scienze della Terra (MIFT), Università di Messina, V.le F.S. d'Alcontres 31, 98166, Messina, Italy
[b] Institute of Nuclear Physics of CAS, v.v.i., Husinec-Řež 130, 250 68, Řež, Czech Republic
[c] INFN, Sezione di Catania, Viale A. Doria 44, 95123, Catania, Italy
[d] Dipartimento Interateneo di Fisica, Università di Bari "Aldo Moro", Via G. Amendola 173, 70125 Bari, Italy

ARTICLE INFO

Handling Editor: Prof. L.G. Hultman

Keywords:
Graphene oxide
Laser ablation
Ablation yield
Time-of-flight
Mass spectrometry

ABSTRACT

During the laser ablation of a graphene oxide target in the vacuum with a 1064 nm ns laser at about 60 J/cm^2 fluence, the ablation dynamics and molecular emission have been investigated using a quadrupole mass spectrometer (QMS), time-of-flight measures of the emitted ions and dedicated spectroscopies. The plasma characterization has been obtained giving providing the involved ion species and charge states, and the average temperature and density. Increasing the laser fluence the ablation yield, the plasma density and temperature, the velocity of the emitted particles and the emitted mass yields increase. Due to the laser heating a graphene oxide reduction is also observed. The oxygen is emitted as elemental and as part of different functional groups. A strong dehydration and dehydrogenation occur due to the laser pulse energy deposition, testifying the high content of water and hydrogen possessed by graphene oxide.

1. Introduction

The laser ablation of carbon-based materials has attracted much attention because of its utility in the deposition of thin films, generation of nanostructures and carbon-dots, synthesis of diamond-like structures, generation of carbon clusters and highly ionized carbon atoms, oxidation and reduction of carbon surfaces [1–5]. In particular, the laser irradiation of graphene oxide (GO) foils in air, gases or vacuum is having interest for the possibility to enhance or to reduce the oxygen concentration, to remove the water and functional oxygen groups (hydroxyl, carbonyl, carboxyl, epoxy) and to generate carbon atoms aggregations [6,7].

Despite the extensive investigations about modifications induced in carbon-based materials by the lasers pulse ablation in vacuum, gas or liquids over the past decade, many aspects of these systems are still to be unraveled, not only in the understanding of their chemical and physical properties but also in clarifying the mechanism of occurrence. The temporal velocity profile of ejected atoms from the laser-generated plasma, for example, is an important characteristic in the production of reactive species, determining the structural quality of the deposited film or generated nanostructures. The kinetic energy of the plasma emitted species is a key parameter for controlling many properties of the laser deposited films [8].

The dynamics of the interaction between laser light and carbon-based materials, as well as the detailed aspects of laser-induced plume formation and expansion in different environments, are not fully understood. This is particularly the case for graphene oxide irradiated by intense ns IR laser pulses [9,10]. The study of the spatial and temporal distribution of the ablated species during the initial stage of plasma ejection and expansion improves our knowledge of ablation dynamics.

This paper presents a study of the mass, velocity and angular distribution of ions produced by the laser ablation in the vacuum of graphene oxide using a ns IR laser at the 1064 nm wavelength with fluences of the order of 1–60 J/cm^2. The laser ablation of graphene oxide has been characterized by time-of-flight (TOF) measures of the emitted ions, quadrupole ejected species mass detection, crater depth profile, scanning electron microscopy (SEM) and Energy dispersive X-rays analysis (EDX) of the pristine and the laser irradiated GO at various laser fluences. The dependence of the observed emitted masses on the laser fluence is presented and discussed. The time-dependent flow dynamics of plasma plume expansion are also investigated. The obtained results provide direct evidence that small carbon atom aggregates are emitted

* Corresponding author. Dip.to di Scienze Matematiche e Informatiche, Scienze Fisiche e Scienze della Terra (MIFT), Università di Messina, V.le F.S. d'Alcontres 31, 98166, Messina, Italy.
E-mail address: ltorrisi@unime.it (L. Torrisi).

https://doi.org/10.1016/j.vacuum.2023.112031
Received 17 January 2023; Received in revised form 15 March 2023; Accepted 20 March 2023
Available online 21 March 2023

during the plume expansion.

2. Materials and methods

The targets of graphene oxide have been purchased by Graphenea [11]. They consist of sheets of 4 cm diameter, 10–50 μm thick, very uniform, obtained from micrometric platelets of GO dispersed in water. Their composition is: Carbon = 49–56%; Hydrogen = 0–1%; Nitrogen = 0–1%; Sulfur = 2–3%; Oxygen = 41–50% [12]. They have a density of 1.36 g/cm^3, are black in color, electrically insulating, flexible and mechanically very resistant. Laser ablation of a graphene oxide target has been carried out in a vacuum chamber (base pressure $<10^{-6}$ mbar) combined with an ion-collector (IC), using a Faraday cup with suppression grid for the ion TOF measurements, and equipped with a mass quadrupole spectrometer (Pfeiffer Prisma Vacuum QMS 220). The TOF spectroscopy uses a flight distance of 100 cm and a fast storage oscilloscope (Tektronix 2 GHz, 20 GS/s). A visible fast CCD camera (PixeFly PCO.Imaging 200 SX) triggered by the laser pulse has been employed to photograph the plasma plume emission with a minimum exposition time of 1 μs. The CCD camera was placed at a 90° angle with respect to the normal direction to the target surface together with a suitable optic that permits to focalize on the plasma plume.

QMS uses a secondary electron multiplier (Sem) to have high sensitivity (below 1 ppm), to detects masses from 1 up to 300 amu with a mass sensitivity lower than 1 amu [13]. QMS is positioned 80 cm far from the target and it does not see the direct emission from the target but only the residual gas component present in the scattering chamber just before and after the laser pulse irradiation. The gas is removed by a fast turbomolecular vacuum pump acting on about 25-L vacuum chamber.

A Q-switched Nd:Yag laser operating at 1064 nm, with a 3 ns pulse duration (full width at half maximum-FWHM), (1–900) mJ pulse energy and an 1 cm output beam (Litron laser), is employed. The laser beam is focused on the target surface to about 1 mm^2 spot size using a 50 cm focal length lens placed externally to the vacuum chamber. The focused laser beam is employed to irradiate the target using a glass window for the beam entrance. Generally, the incidence angle was maintained at 0°; only for the IC measurements the incident angle was 45°, with the normal target directed towards the IC detector, in order to correctly measure the maximum ion energy. Laser operates in single pulse or up to a 10 Hz repetition rate [14].

The target is placed at the centrum of a cylindrical vacuum chamber, and its holder can be moved vertically and rotated around the vertical axis. The maximum laser intensity is about 10^{11} W/cm^2 but in this experiment the maximum used laser intensity has been 2×10^{10} W/cm^2 obtained using a maximum laser fluence of 60 J/cm^2. A scheme of the experimental set up is reported in Fig. 1a, while a photo in Fig. 1b. For the presented measurements, the laser fluence at the target surface has been varied between about 0.6 and 60 J/cm^2.

QMS can be used for measuring the detected secondary electron multiplier current as a function of the mass or as a function of the time fixing the masses of interest. In order to speed up the acquisition of the signal, it has been decided to work in the single laser pulse modality, fixing the masses of interest and following the various signals variations as a function of time. A maximum of only seven or eight masses to follow at a time has been set to speed up the QMS acquisition.

The irradiated GO samples have been analyzed with a surface profiler (Tencor P-10), with a 10 nm depth resolution, in order to measure the ablated crater shape and size and to calculate the ablation yield (i.e. the removed mass per laser pulse).

Attenuated Total Reflectance-Fourier Transform Infrared (ATR-FTIR) spectroscopy has been applied to the pristine GO and to the laser irradiated GO to evince the effect of reduction by laser in vacuum. The spectra have been acquired in the (400–4000) cm^{-1} wavenumber region.

SEM microscopy has been employed with a 20 keV electron beam to study the morphological effects of the laser irradiated surfaces. EDX analysis has been performed using a 5 keV electron beam to detect the Carbon and Oxygen characteristic K_α X-ray fluorescence lines occurring at about 277 and 525 eV, respectively. This spectroscopy has permitted to determine the C/O atomic ratio in order to have a direct measure of the GO reduction after the laser irradiation.

Fig. 2 shows a photo of the used GO sample (a) and a scheme of its structure containing the functional oxygen groups, water molecules and other gases (b) trapped between the graphene platelets.

3. Results and discussion

Using different energies of the laser pulse to irradiate a thick GO sample, it has been possible to measure different ablation yields, i.e. evaluations of removed mass per laser pulse. The removed mass from the crater was measured by the crater shape and size through the surface profile scansion along the crater diameter under optical microscopy.

Fig. 3 reports the comparison of the crater depth profiles obtained in GO using single laser shots at the 60 and 6 J/cm^2 fluences, corresponding to an intensity of 2×10^{10} and 2×10^9 W/cm^2, respectively. The crater observed along its diameter is regular and can be approximated with a half-ellipsoid. The crater volume is about 13.1×10^{-6} cm^3 and 2.63×10^{-6} cm^3 in the two cases, respectively. Assuming the pristine GO density of 1.36 g/cm^3 [15], the ablated mass corresponds to 17.8 μg and 3.6 μg, respectively, which is the value of the measured ablation yield per laser pulse in the two cases. In the (0.6–60) J/cm^2 region, the ablation yield in vacuum (10^{-6} mbar) increases almost

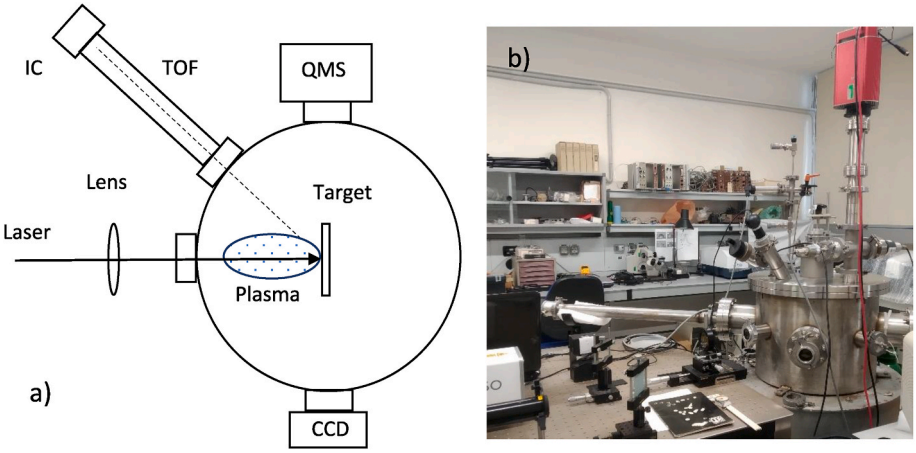

Fig. 1. Scheme of the experimental set-up (a) and its photo (b).

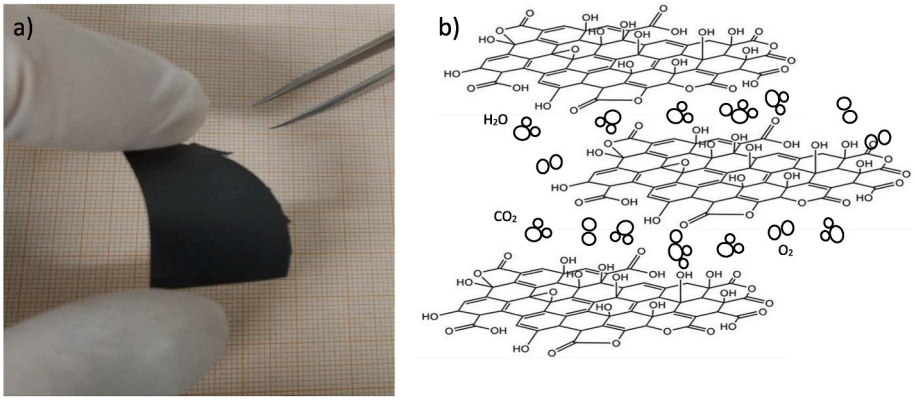

Fig. 2. Photo of the used GO sample (a) and a scheme of its structure containing the functional oxygen groups, water molecules and other gases (b).

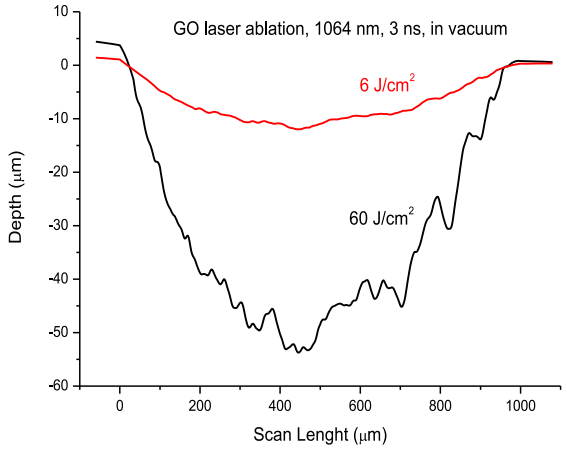

Fig. 3. Crater profile comparison of GO irradiated in vacuum at 6 and 60 J/cm^2 fluence.

linearly with the laser fluence, as reported in the plot of Fig. 4. A slight saturation effect exists towards high laser fluences, probably due to the laser self-absorption effect in the high-density plasma generated in front of the target surface. Furthermore, a yield drop occurs at low fluence, probably due to the effect of the ablation energy threshold at the 1064 nm wavelength [16]. The errors of ablation yield measurements have been evaluated to be of the (8-10) % order. Further and previous measurements have demonstrated that the increment of the laser fluence enhances the plasma temperature, the density and the energy of emitted ions [17].

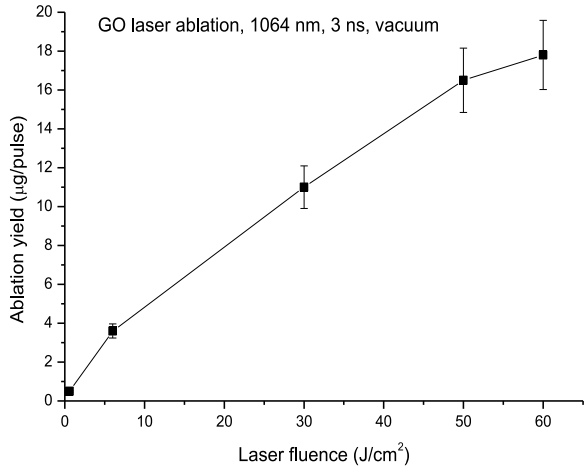

Fig. 4. GO ablation yield in vacuum vs laser fluence.

The obtained results of the ablation yield vs fluence are comparable with those reported in the literature [18,19].

The laser-generated plasma has been characterized overall in terms of ion charge states, average temperature and density. To achieve this, measurements of the maximum ion kinetic energy have been carried out by using a Farady cup connected in the time-of-flight configuration and no optical spectroscopy or Langmuir probe has been employed. A TOF spectrum obtained using a 100 cm flight length and a 600 mJ laser pulse energy is reported in Fig. 5a. It shows a narrow photopeak due to the photon detection during the 3 ns laser shot, used as the starting time, and a large peak due to the detection of the energetic plasma accelerated ions. The faster ions are protons, followed by carbon and oxygen atoms. The large peak represents the convolution of all ions with different charge state. Its front is due to faster ions and its tail to the slower ions. Such ions are accelerated by the electric field developed in the non-equilibrium plasma, and their maximum energy can be measured by the discontinuities present in the large peak shape. By considering the TOF length and the time of faster ions arriving to the IC detector, the maximum proton energy corresponds to 210 eV, that of oxygen ions to about 1340 eV and that of carbon ions to 760 eV. Thus, assuming the maximum ion acceleration of 210 eV per charge state, dividing the measured maximum ion energy by 210 eV, the maximum oxygen charge state corresponds to O^{6+} and that for carbon to C^{4+}. Since oxygen ions with 7+ charge state are not detected, plasma electrons should have energy higher than 138 eV and lower than 739 eV, being the first one the ionization potential of O^{6+} and the second one that of O^{7+}, according to NIST database [20]. Since carbon ions with 5+ charge state are not detected, plasma electrons have energy higher than 64 eV and lower than 392 eV, being the first one the ionization potential of C^{4+} and the second one that of C^{5+}. Thus, we can assume that the maximum electron energy is of about (200–300) eV. Since electrons have a Boltzmann distribution [21], their mean energy should be about one-third of the maximum value i.e. of about (67–100) eV and their approximated average temperature calculable from the equation:

$$< kT > = 2<E>/3 \sim (45–67)\ eV \quad (1)$$

Of course, the temperature depends on the time and space, being higher near to the target surface and during the laser pulse and lower far from the target and successively to the laser pulse [21].

A further characterization of plasma has been performed measuring its visible volume expansion in vacuum during 1 μs from the laser shot. Fig. 5b shows a photo of the visible plasma emission obtained using a fast CCD camera with a 1 μs exposition time triggered by the laser shot. Its shape is ellipsoidal with the major axis directed along the normal to

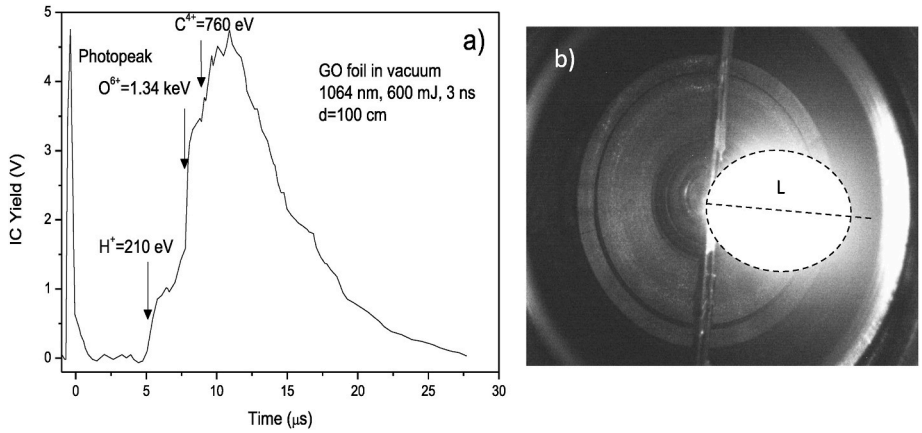

Fig. 5. IC-TOF measurements of plasma-emitted ions (a) and photo of produced plasma with an 1 μs exposition time from the laser shot (b).

the target surface. The angular aperture of the emitted excited species is evaluated of about ±45°. The plasma volume V_0 corresponds to about 4.72 cm^3, thus the plasma mass density at 1 μs expansion time can be evaluated by the ablation yield Y per pulse at 60 J/cm^2 divided the plasma volume:

$$d = Y/V_0 = 17.8\ \mu g/4.72\ cm^3 = 3.77\ \mu g/cm^3 \quad (2)$$

Assuming the carbon to be the main plasma atomic component and using the GO mass density, the plasma atomic density at 1 μs corresponds to about 1.66×10^{18} at/cm^3, in good agreement with the literature [22]. The image reported in Fig. 5b permits also to confirm the average plasma temperature assuming it depends by the plasma adiabatic expansion velocity in vacuum, v_k [21]. In fact, such measured expansion velocity is:

$$v_k = L/dt = 2.6\ cm/1\ \mu s = 2.6 \times 10^4\ m/s \quad (3)$$

Thus, assuming the plasma to be composed mainly by carbon atoms, the corresponding plasma temperature is:

$$kT = m\ v_k^2/\gamma = 51\ eV \quad (4)$$

Being γ the adiabatic coefficient and equal to 1.67. The result given by Eq. (4) is in good agreement with that indicated in Eq. (1).

The QMS spectrometry has been investigated by fixing the masses of greater interest that could be emitted from the laser irradiated GO and recording their yield versus time during a laser irradiation shot. Our attention has been devoted to the different three sets of masses in amu:

First set: 1 (H); 2(H_2); 12 (C); 16(O); 17 (OH); 18 (H_2O); 32 (O_2);

Second set: 24 (C_2); 28 (CO); 29 (COH); 40 (C_2O); 45(CO_2H); 18 (H_2O);

Third set: 12 (C); 24 (C_2); 36 (C_3); 48 (C_4); 60(C_5); 72(C_6); 84(C_7); 18 (H_2O);

The first set was devoted to have evidence of water and simple oxygen molecules emission. The second set was devoted to detect some functional oxygen groups, and the third set to evince the emission of agglomerated small carbon atoms. The water was always revealed as reference peak.

The spectra shown in Figs. 6–8 are referred to the three sets of QMS detected masses vs time. The first set, shown in Fig. 6, suggests that water is the emitted mass at the largest amount, followed by the OH and O species. The emission of O_2, and H represent quantities of about one order of magnitude lower than water emission. The minimum molecular emission yield is that relative to H_2. The plasma duration corresponds to about five times the laser pulse width, as measured using both a very fast Si photodiode and measuring the photopeak width from the IC-TOF measurements. Thus, it is of about 15 ns (FWHM), but the residual gas in the chamber has a duration of about 2–3 s as measured by the QMS spectra.

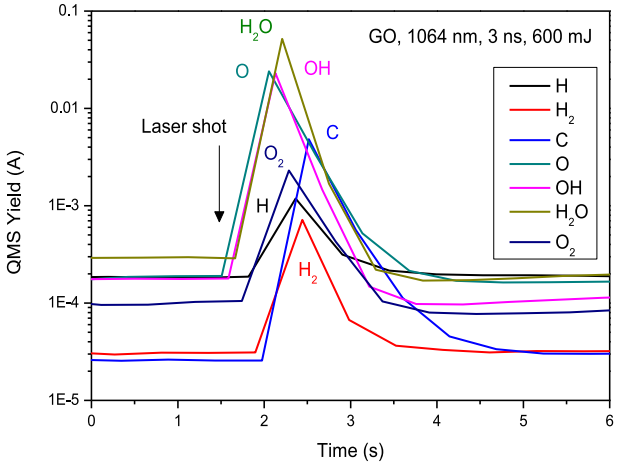

Fig. 6. QMS emission yield of the first set of selected masses during one shot of GO laser ablation.

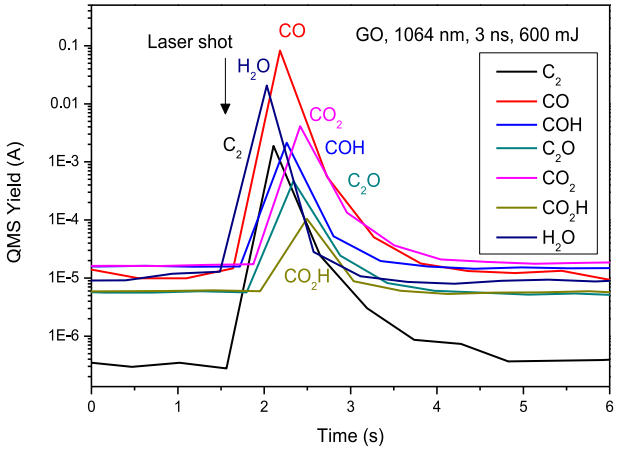

Fig. 7. QMS emission yield of the second set of selected masses during one shot of GO laser ablation.

The second set, shown in Fig. 7, shows some functional oxygen groups emitted, such as the hydroxyl (C–OH), the epoxy (C–*O*–C), the carbonyl (C═O) and the carboxyl (O–C═O), the water and the carbon

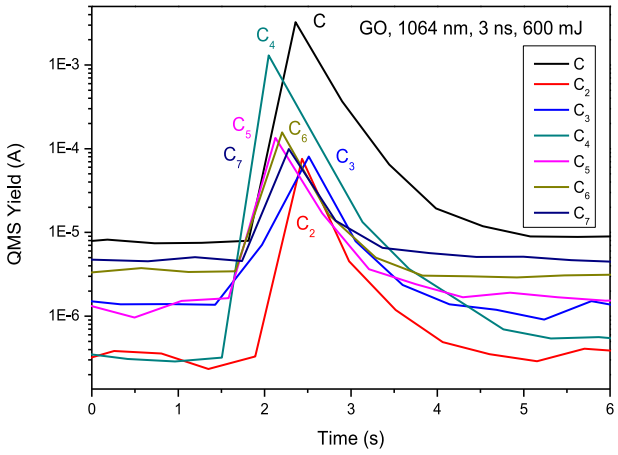

Fig. 8. QMS emission yield of the third set of selected masses during one shot of GO laser ablation.

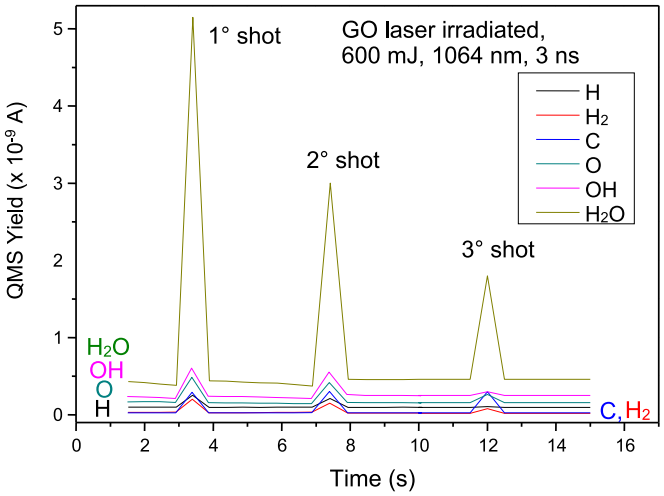

Fig. 9. QMS yield versus time for the first six masses of interest using three successive laser shots.

dioxide emission, in agreement with the literature [23]. The CO is the higher emitted mass, followed by the H_2O. The emissions of CO_2, COH, C_2 and C_2O, that represent quantities of about one order of magnitude lower than water emission, follow. The minimum molecular emission yield is that relative to CO_2H. Also, for these species the detection time in the vacuum chamber has duration of about 2–3 s from the laser shot.

The third set, shown in Fig. 8, indicates the emission of small carbon atoms agglomerations. The C atomic mass represents the emitted mass at the largest quantity, as expected, but its yield is about one order of magnitude lower with respect to that of the water emission. It is followed by the C_4 atomic group. C_2, C_3, C_5, C_6 and C_7 masses are emitted with about one order of magnitude lower with respect to the C emission. Also, for these species the detection time has duration of about 2–3 s from the laser shot. The carbon nucleation in the laser-generated plasma is reported in the literature and can also reach the form of C_{60} fullerene [24].

The comparison of the measurements presented in Figs. 6–8 indicate that the largest mass species quantities, that are laser removed from GO, are represented by the QMS signal higher that about 0.01 A, corresponding to the masses of H_2O, OH, O and CO. Thus, GO contains high amount of water molecules, functional groups of oxygen and oxygen atoms.

Reported data confirm that the irradiated GO is ablated and transformed in plasma, i.e. in vapor of ionized atoms. The residual material near to the crater edge has been heated by the IR laser. In fact, the laser transfers energy to the removed atoms and molecules but also to the GO target, thus reducing its oxygen content, in agreement with the literature data [17,25].

This phenomenon has been also demonstrated by our investigations performed using ATR-FTIR and EDX spectroscopies. The repetitive laser pulse irradiation on the previous GO crater enhances its depth and produces emission of other ablated atoms and molecules which can be analyzed on-line by QMS. Measurements demonstrated that the successive irradiation decreases the amount of hydrogen, water, oxygen and functional groups of oxygen, enhancing the carbon emission and demonstrating that GO is laser reduced by the first laser shot and by the successive, according to the literature [5].

Fig. 9 shows the QMS spectra vs time using three successive laser shots on the same crater. It is possible to observe the high decreasing of the water, OH hydroxyl group and O atoms and the near constancy of the carbon atom emission. Such result indicates that the IR radiation produces not only mass ablation but also a significant heating of the material around to the crater, thus reducing the GO material near to the crater zone and enhancing in this zone the carbon relative concentration, in agreement with the literature [26].

In fact, the diffusion length of the heat in rGO, L_D, is of the orders of several microns. It can be evaluated by the thermal conductivity of rGO (~2500 W/m K), its density (~1.6 g/cm^3), its specific heat (~500 J/kg K) and plasma duration τ_p. Assuming the plasma duration to be about 5 times the laser pulse duration, the diffusion length evaluation is:

$$L_D = \sqrt{D\tau_p} = \sqrt{\frac{k}{\rho c_s}\tau_p} \approx 6.8\ \mu m \tag{5}$$

The effect of the laser reduction of GO during the QMS analysis, relative to the spectra of Fig. 9 can be observed in the plot data of Fig. 10 reporting the QMS net peak yield, with the subtracted background, for the first six masses of interest and for three consecutive laser shots.

Although the mass quadrupole analysis itself indicates the reduction of the GO irradiated in vacuum, further verifications of this reduction have been sought by analyzing the inner wall and the edges of the laser craters irradiated with the two spectroscopic techniques reported below, the ATR-FTIR and the EDX spectroscopies.

Fig. 11a shows an ATR-FTIR transmittance spectra comparison, in the (400–4000) cm^{-1} wavenumber region, between the pristine GO foil and the residual material at the edge of the crater in the reduced GO (rGO) obtained by laser irradiating GO at the 600 mJ pulse energy (60 mJ/cm^2 laser fluence). Fig. 11 b shows a SEM image of the laser crater

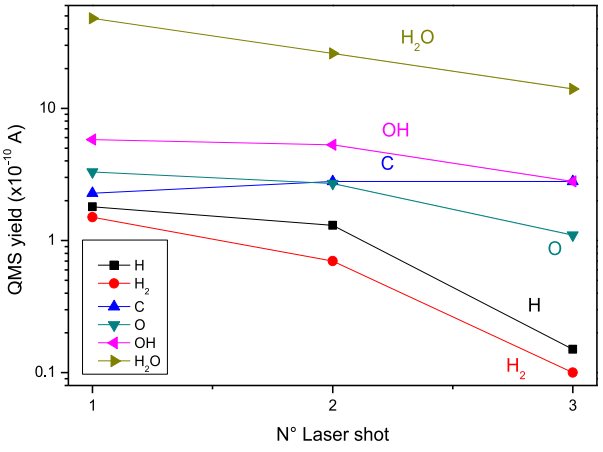

Fig. 10. QMS yield vs laser hot for the first six masses of interest.

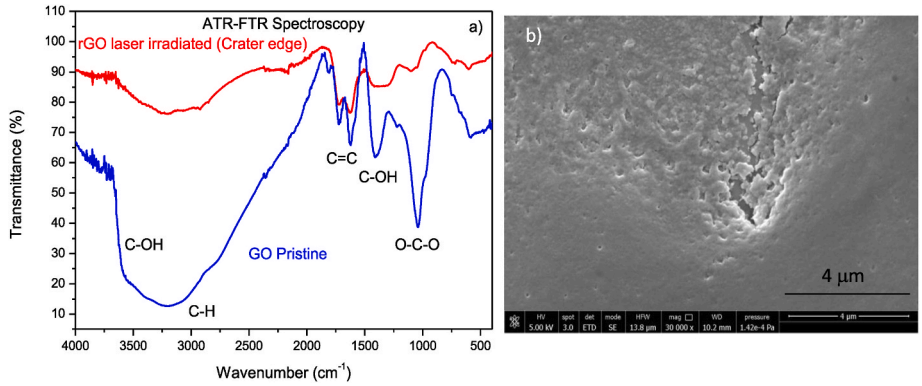

Fig. 11. ATR-FTIR spectra for pristine GO and laser irradiated rGO.

edge where the ATR-FTIR analysis has been performed. In this region, the IR transmittance is lower in the pristine GO, due to the absorbance of functional oxygen groups, and is higher in the laser treated GO, rich in the carbon content. In fact, it is possible to observe that the laser reduced GO spectrum shows a strong reduction of O–C–O, C–OH, C═C, and C–H groups which, instead, are strongly contained in the pristine GO. The obtained results are in good agreement with the literature [27,28].

For further evidence of the laser reduction of GO, residual material around to the ablated crater region is visible from the EDX spectroscopy. Fig. 12 compares the EDX spectra in pristine GO and laser reduced GO, analyzed near to the crater zone. Normalizing the spectra to the carbon Kα line (277 eV), the characteristic X-ray Kα line of oxygen (525 eV) appears strongly reduced in the rGO material. A quantitative analysis indicates that the C/O atomic ratio of 1.6 in the pristine GO increases up to 3.1 in the high reduced material, in good agreement with the literature [29].

Increasing the laser fluence (J/cm^2) the effect of GO reduction in vacuum increases, in agreement with our previous investigations reported in the literature [5].

4. Conclusions

The laser ablation of graphene oxide at the 1064 nm wavelength, with the 3 ns pulse duration and the 0.6–60 J/cm^2 fluence has been investigated using a quadrupole mass spectrometer and different optical spectroscopies. The carbon-based plasma is rich in hydrogen and oxygen ions, testifying the high amount of these elements in the GO matrix. The obtained plasma has a temperature and density evaluated of about 50–60 eV and 1.7 × 10^{18} at/cm^3, respectively.

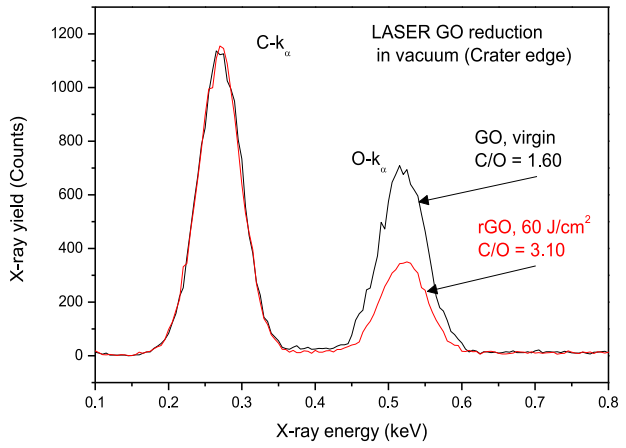

Fig. 12. EDX spectra comparison of GO and laser reduced rGO (crater edge material).

The mass spectra show characteristic peaks of the atomic elements and molecules chemically bonded and trapped into the GO lamellar structure, such as the functional groups of oxygen, the water, and the absorbed gases such CO_2, hydrogen, and other compounds that can be formed in the hot laser-generated plasma. Also, groups of carbon atoms are emitted from the ablation, measured from single C up to 7-C but probably also heavier carbon aggregated will be present but not detectable with our spectrometer.

The fast laser ablation removes a GO mass, which is of the order of 18 μg at the high fluence of 60 J/cm^2, it heats the GO target inducing its reduction in the vacuum, in agreement with the literature.

In fact, near the crater edges, the C/O atomic ratio increases from about 1.6 up to about 3.1 and more, depending on the employed laser fluence and by the number of laser shots hitting the target.

Increasing the laser fluence, the reduction increases and the emitted masses too. The laser-ablated plume is characterized by an axial expansion of the plume in vacuum, i.e., strictly along a direction perpendicular to the target surface. The used QMS is not positioned in front of the target surface to be not influenced by the highly ionized species but it is positioned laterally, permitting the detection of the recombined ions in form of gas at a given pressure produced in the high vacuum chamber. Thus, QMS detection does not concern the direct plasma ionized atoms but the nearly thermalized species produced by the atom collisions in the expanding plasma. The compositional variation in the plume arises from the different atomic emission from the irradiated GO or rGO and indicates that significant water and functional oxygen groups are emitted leaving the residue material greatly reduced.

The obtained results can be employed to treat thin GO sheets and to modify their macroscopic structure using cover masks, to drill holes, to reduce GO using low laser fluences, to prepare membranes and microfilters, and more. Sometimes, however, the associated reduction in GO due to the used IR radiation may not be desired for the chemical and physical properties of rGO, very different from GO. In such cases, to modify the morphology and thickness of the GO films, it is advisable to use UV lasers which promote more photochemical effects and bond breakings and not photothermal effects, as current ongoing investigations are demonstrating.

CRediT authorship contribution statement

L. Torrisi: Writing – original draft, Supervision, Investigation, Conceptualization. **M. Cutroneo:** Investigation. **L. Silipigni:** Investigation. **A. Torrisi:** Investigation, Data curation.

Declaration of competing interest

The authors declare that they have no known competing financial interests or personal relationships that could have appeared to influence the work reported in this paper.

Data availability

No data was used for the research described in the article.

Acknowledgement

Authors thank the INFN, Gr. V, for the useful support given to the project CIMA, realized with the collaboration of INFN, Catania Section and University of Messina (Italy) and Nuclear Physics Institute of Czech Republic. This publication was supported by OP RDE, MEYS, Czech Republic under the project CANAM OP,CZ.02.1.01/0.0/0.0/16_013/0001812.

References

[1] Z. Geretovszky, T. Haraszti, T. Szörényic, F. Antoni, E. Fogarassy, Morphological study of PLD grown carbon films, Appl. Surf. Sci. (2003) 566–574, 208-209.
[2] H. Yu, X. Li, X. Zeng, Y. Lu, Preparation of carbon dots by non-focusing pulsed laser irradiation in toluene, Chem. Commun. 52 (4) (2016) 819–822.
[3] A. Mangione, L. Torrisi, A. Picciotto, F. Caridi, Physical characterization of pulsed laser deposition of diamond-like nanostructures, Czech. J. Phys. 56 (2006) B534–B541.
[4] L. Torrisi, A. Torrisi, Advantages to use graphene oxide thin targets in forward ion acceleration using fs lasers, Contrib. Plasma Phys. 62 (2022) 1–12, e202200037.
[5] L. Torrisi, L. Silipigni, M. Cutroneo, Radiation effects of IR laser on graphene oxide irradiated in vacuum and in air, Vacuum 153 (2018) 122–131.
[6] S. Mortazavi, M. Mollabashi, R. Barri, K. Jones, J.Q. Xiao, R.L. Opila, S.I. Shah, Modification of graphene oxide film properties using KrF laser irradiation, RSC Adv. 23 (2018) 12808–12814.
[7] L. Torrisi, L. Silipigni, M. Cutroneo, Laser effects on graphene oxide irradiated in high vacuum, Rad. Eff. and Def. in solids 173 (1–2) (2018) 73–84.
[8] A. Hu, J. Sanderson, Y. Zhou, W.W. Duley, Formation of diamond-like carbon by fs laser irradiation of organic liquids, Diam. Relat. Mater. 18 (5–8) (2009) 999–1001.
[9] A. Torrisi, L. Velardi, A. Serra, D. Manno, L. Torrisi, L. Calcagnile, Graphene oxide modifications induced by excimer laser irradiations, Surf. Interface Anal. 54 (2022) 567–575.
[10] L. Torrisi, M. Rosinski, M. Cutroneo, A. Torrisi, J. Badziak, A. Zaras-Szydlowska, P. Parys, Target normal sheath ion acceleration by fs laser irradiating metal/reduced graphene oxide targets, J. Inst. Met. 15 (1) (2020) 1–15. C03056.
[11] Graphenea, actual website, Dedicated Graphene Foundry – Graphenea, 2023.
[12] Graphenea,graphene oxide, actual website, Graphene Oxide – Graphenea, 2023.
[13] QMS 220, Pfeiffer-Vacuum, actual website, PTM06241111.en.pdf (pfeiffer-vacuum.com), 2023.
[14] Litron laser, actual website, Litron Lasers - Designed for Research, Engineered for Industry, 2023.
[15] L. Torrisi, M. Cutroneo, A. Torrisi, L. Silipigni, Measurements on five characterizing properties of graphene oxide and reduced graphene oxide foils, Phys. Status Solidi 219 (6) (2022), 2100628.
[16] L. Torrisi, A. Borrielli, D. Margarone, Study on the ablation threshold induced by pulsed lasers at different wavelengths, *Nucl. Instrum. Methods Phys. Res.* B 255 (2007) 373–379.
[17] L. Torrisi, M. Cutroneo, A. Torrisi, G. Salvato, E. Proverbio, L. Silipigni, Reduction of graphene oxide foils by IR laser irradiation in air, J. Inst. Met. 15 (1) (2020) 1–15. C03006.
[18] M.R. Marks, Z. Hassan, K.Y. Cheong, Ultrathin wafer pre-assembly and assembly process technologies: a review, Crit. Rev. Solid State Mater. Sci. 40 (2015) 251–290.
[19] M.D. Shirk, P.A. Molian, Ultra-short pulsed laser ablation of highly oriented pyrolytic graphite, Carbon 39 (2001) 1183–1193.
[20] NIST Ionization potentials, actual website, NIST: Atomic Spectra Database - Ionization Energies Form, 2023.
[21] S. Eliezer, The Interaction of High-Power Lasers with Plasmas, IOP, Bristol, 2002.
[22] S.S. Harilal, C.V. Bindhu, R.C. Issac, V.P.N. Nampoori, C.P.G. Vallabhana, Electron density and temperature measurements in a laser produced carbon plasma, J. Appl. Phys. 82 (5) (1997) 2140–2146.
[23] K. Krishnamoorthy, M. Veerapandian, K. Yun, S.J. Kim, The chemical and structural analysis of graphene oxide with different degrees of oxidation, Carbon 53 (2013) 38–49.
[24] S. Iijima, T. Wakabayashi, Y. Achiba, Structures of carbon soot prepared by laser ablation, J. Phys. Chem. 100 (1996) 5839–5843.
[25] Y. Zeng, T. Li, Y. Yao, T. Li, L. Hu, A. Marconnet, Thermally conductive reduced graphene oxide thin films for extreme temperature sensors, Adv. Funct. Mater. 29 (27) (2019), 1901388.
[26] S. Hun, Thermal reduction of graphene oxide, Physics and applications of graphene-experiments 19 (2011) 73–90.
[27] S.N. Alam, N. Sharma, L. Kumar, Synthesis of graphene oxide (GO) by modified hummers method and its thermal reduction to obtain reduced graphene oxide (rGO), Graphene 6 (2017) 1–18.
[28] F.T. Johra, W.G. Jung, Hydrothermally reduced graphene oxide as a supercapacitor, Appl. Surf. Sci. 357 (2015) 1911–1914.
[29] N. Bano, I.H. Asghar, A. El-Naggar, A.A. Albassam, Reduced graphene oxide nanocomposites for optoelectronics applications, Appl. Phys. A 125 (3) (2019) 125–215.